Journal of Pharmaceutical Sciences xxx (2016) 1-7

Contents lists available at ScienceDirect

Journal of Pharmaceutical Sciences

journal homepage: www.jpharmsci.org

Pharmaceutics, Drug Delivery and Pharmaceutical Technology

Lubricant-Induced Crystallization of Itraconazole From Tablets Made of Electrospun Amorphous Solid Dispersion

Balázs Démuth [1], Attila Farkas [1], Attila Balogh [1], Karolina Bartosiewicz [1], Barnabás Kállai-Szabó [2], Johny Bertels [3], Tamás Vigh [3], Jurgen Mensch [3], Geert Verreck [3], Ivo Van Assche [3], György Marosi [1, *], Zsombor K. Nagy [1, *]

[1] Department of Organic Chemistry and Technology, Budapest University of Technology and Economics, Budapest 1111, Hungary
[2] Department of Pharmaceutics, Semmelweis University, Budapest 1091, Hungary
[3] Drug Product Development, Janssen R&D, Beerse 2340, Belgium

ARTICLE INFO

Article history:
Received 23 December 2015
Accepted 28 April 2016

Keywords:
oral drug delivery
amorphous
solid dispersion
dissolution
crystallization
nanotechnology
tableting
chemical stability
Raman spectroscopy

ABSTRACT

Investigation of downstream processing of nanofibrous amorphous solid dispersions to generate tablet formulation is in a quite early phase. Development of high speed electrospinning opened up the possibility to study tableting of electrospun solid dispersions (containing polyvinylpyrrolidone-vinyl acetate and itraconazole [ITR] in this case). This work was conducted to investigate the influence of excipients on dissolution properties and the feasibility of scaled-up rotary press tableting. The dissolution rates from tablets proved to be mainly composition dependent. Magnesium stearate acted as a nucleation promoting agent (providing an active hydrophobic environment for crystallization of ITR) hindering the total dissolution of ITR. This crystallization process proved to be temperature dependent as well. However, the extent of dissolution of more than 95% was realizable when a less hydrophobic lubricant, sodium stearyl fumarate (soluble in the medium), was applied. Magnesium stearate induced crystallization even if it was put in the dissolution medium next to proper tablets. After optimization of the composition, scaled-up tableting on a rotary press was carried out. Appropriate dissolution of ITR from tablets was maintained for 3 months at 25°C/60% relative humidity. HPLC measurements confirmed that ITR was chemically stable both in the course of downstream processing and storage.

Introduction

Formation of amorphous solid dispersion has been frequently applied over the last 2 decades in order to enhance the bioavailability of poorly water soluble drugs (Biopharmaceutical Classification System II and IV class). The processes of spray drying and melt extrusion have been examined thoroughly and have become well-described with years.[1-3] The most relevant features of solid dispersions are in fact the enhancement of dissolution and the question is whether the enhanced dissolution properties can be maintained in final products (i.e., tablets) or not. Dissolution from tablets is usually slower due to the disintegration step and prolonged wetting. Meanwhile, the extent of dissolution usually does not change significantly with tablets[4-7] although both increases[8-10] and decreases[6,7,11] were reported. Faster dissolution rates from tablets can be attributed either to a step decreasing the particle size before tableting[12] or to the fact that gelling of the polymer is less probable in tablets if each solid dispersion particle is dispersed completely allowing rapid wetting.[10]

Another very important aspect is the maintenance of supersaturation during dissolution from a tablet, which can be challenging. Rapid dissolution from amorphous solid dispersions enables a supersaturated state of the active pharmaceutical ingredient (API), which can generate higher bioavailability, but it might initiate precipitation.[13] Therefore, amorphous solid dispersions with slower dissolution rates are sometimes more useful as they can prolong the time of supersaturation at a lower level.[14,15] In order to predict supersaturation and precipitation phenomena under *in vivo* circumstances, some *in vitro* models have been developed.[14,16,17] Tableting can enable adjusting the dissolution rate through appropriate compression force and composition, thus maximizing bioavailability.[18]

Conflicts of interest: The authors report no conflicts of interest.

* *Correspondence to:* Zsombor K. Nagy (Telephone: +36-1463-1424; Fax: +36-1463-3648) and György Marosi (Telephone: +36-1463-1424; Fax: +36-1463-1150).
E-mail addresses: zsknagy@oct.bme.hu (Z.K. Nagy), gmarosi@mail.bme.hu (G. Marosi).

http://dx.doi.org/10.1016/j.xphs.2016.04.032
0022-3549/

The chance for amorphous solid dispersions to achieve better bioavailability depends on the maintenance of supersaturation. Polymers that are able to form H-bonds with the API can usually prolong the supersaturated state realizing a higher bioavailability.[15] Vandecruys et al.[19] screened some formulation excipients (with 25 drug candidates) that affect supersaturation by various mechanisms. Surfactants and hydroxypropyl-ß-cyclodextrin were found to be the best at augmenting the extent of supersaturation (enhancing the solubility), while pharmaceutical polymers (e.g., hydroxypropyl methylcellulose and polyvinylpyrrolidone) were more useful at maintaining the stability of supersaturated state but did not create a high supersaturation extent. However, disadvantageous changes generated by excipients (through physical or chemical interactions with the drug) have been reported too.[20] In one case, API, having low dose, was partly bound to microcrystalline cellulose that led to a dissolution failure.[21] Magnesium stearate (MgSt), which is of particular interest in this work, decreased antibacterial activity of cetylpyridinium chloride by adsorbing it onto the stearate anion.[22]

The industrial feasibility of electrostatic spinning, which is a gentle way to produce amorphous solid dispersions and solutions, is promising. Processes derived from the basic technology are vividly investigated for versatile pharmaceutical applications: melt electrospinning,[23,24] coaxial electrospinning,[25,26] triaxial electrospinning,[27,28] and so on. However, downstream processing (which is related to scaling-up of the technology) of nanofibers to generate tablet formulations has not been studied. Because its pharma-compatible scaled-up technology, called high speed electrospinning, is published,[29] detailed investigation of its downstream processing became the next step. The objective of this article was manifold. First, it was intended to develop tablet formulation, based on electrospun fibers, from which the release of itraconazole (ITR) is fast and complete. Furthermore, a crystallization induced by MgSt was investigated in detail. It was of great importance to carry out rotary press tableting with optimized composition (another lubricant sodium stearyl fumarate (SSF) was applied). This is the first time, to the authors' best knowledge, that scaled-up tableting of an electrospun material (EM) has been accomplished using a rotary press. Finally, but not the least, it was investigated if physical and chemical stability of ITR in tablets could be maintained. Demonstration of large-scale tableting of physically and chemically stable electrospun fibrous amorphous solid dispersion, formed with high throughput method, may open up new formulation possibilities for pharmaceutical scientists.

Materials and Methods

Materials

ITR, MgSt, and SSF were provided by Johnson & Johnson Pharmaceutical Research and Development (Beerse, Belgium). Aerosil® 200 was purchased from Evonik Industries (Essen, Germany). Microcrystalline cellulose (MCC, Vivapur® 200) was given by JRS Pharma (Rosenberg, Germany). Mannitol (Pearlitol® 400DC) was a kind gift from Roquette Pharma (Lestrem, France). PVPVA64 and Kollidon® CL were supplied by BASF (Ludwigshafen, Germany).

Preparation of EM by High Speed Electrospinning

EM was prepared according to the description provided by Nagy et al.[29] The high speed electrospinning of the solution with PVPVA64 (60%) and ITR (40%) in dichloromethane-ethanol (2:1) was performed under the following conditions: 50 kV voltage, 40,000 rpm spinneret rotational speed, 1500 mL/h feeding rate, and ambient temperature. Further information and basic characterization can be found in the aforementioned article.

Preparation and Characterization of Tablets

Tablets were compressed on a Huxley Bertram hydraulic compaction simulator equipped with 9.5-mm flat-face punches and instrumented die. The compression profiles were created with the compaction simulator software for a Courtoy Modul S press (B-tooling). Hardness was measured on an ERWEKA TBH30 hardness tester with 3 tablets. Tensile strength was calculated from hardness as follows:

$$T = \frac{2 \cdot H}{\pi \cdot t \cdot d}$$

where T is the tensile strength, H is hardness, t is thickness of tablets, and d is the width of the tablet. Friability was measured on ERWEKA TAR20 friability tester after 4 min at 25 rpm on 10 tablets. Porosity was calculated as follows:

$$P = 1 - \frac{\frac{m}{100 \cdot \pi \cdot \left(\frac{d}{2}\right)^2 \cdot t}}{\rho}$$

where P is the porosity, m is the mass of the tablet, d is the diameter of the punch, t is the thickness of the tablet, and ρ is the true density of the blend. True densities of the blends were determined on an Accupyc 1330 helium pycnometer (Micromeritics, Atlanta, GA). Disintegration time was determined on an ERWEKA ZT71 disintegration tester in tap water at 37°C with 3 tablets.

Disintegration time and tensile strength data were evaluated with Statistica 12 software (Tulsa, OK). Optimization was carried out with the same software (desirability function). It optimizes the dependent variables so the disintegration time is minimal and tensile strength is maximal. The software analyzes the whole studied area and chooses the point which is the best for both dependent variables (with same importance).

Dissolution Test and Flask Measurements

Dissolution tests were executed under non-sink conditions with 3 parallel measurements on a DISTEK 2100B dissolution tester. Measurement parameters were as follows: 900 mL of 0.1 N HCl, United States Pharmacopeia Dissolution Apparatus 2, 100 rpm paddle speed, variable temperature (37 ± 0.5°C or room temperature 22°C). Manual sampling was applied and the absorption of the samples was measured on an Agilent ultraviolet (UV) spectrophotometer (Agilent, Santa Clara, CA) at 254 nm. Each tablet contained 50 mg of ITR. A calibration was prepared for the determination of ITR concentration. For the stock solution, the crystalline ITR was dissolved in ethanol and then filled up with pH1 acid. The ratio of the 2 solvents was as follows: ethanol:pH1 1:9. Ethanol did not cause any shift or alteration in the UV spectrum of ITR. The calibration range was 1-50 mg/L.

Flask measurements were carried out in lockable flasks with a volume of 900 mL at 4 different temperatures (22°C, 32°C, 37°C, and 45°C). The neat EM, blend, or tablet equal to 50 mg ITR along with stir bars was put into the flask (filled with 900 mL of 0.1 N HCl) located on a magnetic stirrer. After half an hour of stirring (500 rpm), absorption was measured on an Agilent UV spectrophotometer at 254 nm. If it was necessary, temperature was set for the solution prior to addition of tablets.

Table 1
Composition of Tablets

Variable	Material	Blend 1 (F1-F3)	Centre Blend (F4-F6)	Blend 2 (F7-F9)
Composition	EM (mg)	125 (25%)	125 (22.4%)	125 (19.5%)
	MCC (mg)	157 (31.5%)	183 (32.8%)	219 (34.2%)
	Mannitol (mg)	157 (31.5%)	183 (32.8%)	219 (34.2%)
	Kollidon CL (mg)	50 (10%)	56 (10%)	65 (10%)
	Aerosil 200 (mg)	5 (1%)	5.6 (1%)	6.5 (1%)
	Magnesium stearate (mg)	5 (1%)	5.6 (1%)	6.5 (1%)

Raman Spectrometry

After dissolution tests the filtered solid residues were investigated with Raman spectrometry to determine the quality of undissolved or precipitated materials. The point measurements were performed using Horiba Jobin-Yvon LabRAM-type microspectrometer with external 785 nm diode laser source and Olympus BX-40 optical microscope. The laser beam was focused by an objective of 50× to the fine particles to acquire Raman spectrum. The confocal hole of 1000 μm and 950 groove/mm grating monochromator were used in confocal system and for light dispersion. The spectral range of 460-1680 cm^{-1} was detected as the relevant range with 3 cm^{-1} resolution. Each spectrum was collected at 30 s and 3 spectra were averaged per point.

Polarized Light Microscopy

The samples filtered after dissolution test were investigated by Amplival, Carl Zeiss Jena polarized light microscope (Jena, Germany).

Scaled-Up Tableting on a Rotary Press

Scaled-up tableting was carried out on a Kambert KMP-8 table top rotary press (Ahmedabad, India) equipped with eight 8 × 16 mm oblong punches. In total, 9 and 23 rpm were applied as tableting speed. The optimized formulation (76.25% fillers fraction) with 1.5% SSF as lubricant was used for scaled-up tableting.

Storage

Tablets were kept in a Binder KBF 720 climate chamber at 25°C/60% relative humidity (RH) in open holders.

Table 2
Factors of the Performed Experimental Design and the Obtained Results ($n = 3$)

Batch Number	Compression Force (kN)	Fillers Fraction (%)[a]	Tensile Strength (N/mm^2)	Disintegration Time (s)
F1	3.0	71.4	0.67 ± 0.08	98 ± 9
F2	4.5	71.4	1.37 ± 0.10	289 ± 80
F3	6.0	71.4	2.23 ± 0.03	832 ± 56
F4	3.0	74.6	0.60 ± 0.01	38 ± 4
F5	4.5	74.6	1.20 ± 0.05	226 ± 24
F6	6.0	74.6	1.96 ± 0.12	343 ± 105
F7	3.0	77.8	0.52 ± 0.02	25 ± 4
F8	4.5	77.8	1.03 ± 0.03	93 ± 12
F9	6.0	77.8	1.84 ± 0.09	363 ± 15
OT	6.0	76.25	1.94 ± 0.04	337 ± 36

[a] $\left(\frac{m_{fillers}}{m_{fillers}+m_{EM}}\right) \times 100$.
OT, optimized tablets.

HPLC Studies

Maintenance of chemical stability of ITR in the tablets during storage period was determined by analyzing the decomposition byproducts using RP-HPLC (Agilent 1200 series LC System). The HPLC method of Ph. Eur. 5.0 for ITR was adopted. Accordingly, a gradient elution of 27.2 g/L tetrabutylammonium hydrogen sulfate and acetonitrile was performed at a flow rate of 1.5 mL/min and 25°C started at 20% acetonitrile, increased linearly to 50% over 20 min and maintained for 5 min, then returned to the initial composition over 5 min. The UV detection wavelength was set to 225 nm. The samples were dissolved in a mixture of equal volumes of methanol and tetrahydrofuran obtaining a 1 mg/mL solution of ITR, and 10 μL of this stock solution was injected onto the column (Agilent Zorbax Eclipse C18 column [3.5 μm; 100 × 4.6 mm]). The amount of degradation products was determined based on the peak areas. The chromatography tests were done in duplicate.

Results and Discussion

An experimental design with independent variables of compression force and composition of tablets was carried out in order to optimize the disintegration time and tensile strength. Composition of tablets varied in the ratio of EM to fillers (Table 1), while compression force was set to 3, 4.5, and 6 kN for each composition.

The design of experiments and obtained results are presented in Table 2. Optimal point was found to be at 76.25% fillers fraction and 6 kN compression force (both independent variables had the same importance).

The Dissolution Tests

Dissolution tests were carried out with certain batches of the experimental design in order to assess the *in vitro* drug dissolution (Fig. 1). All curves depict the mean of 3 parallel measurements, and deviation is not displayed to avoid clutter (but deviations stayed under 5%).

Dissolution rates in the first 10 min were quite similar for F7 and F9 tablets (containing the same blend). Interestingly, dissolution of F9 tablets was significantly faster than that of F1 tablets although

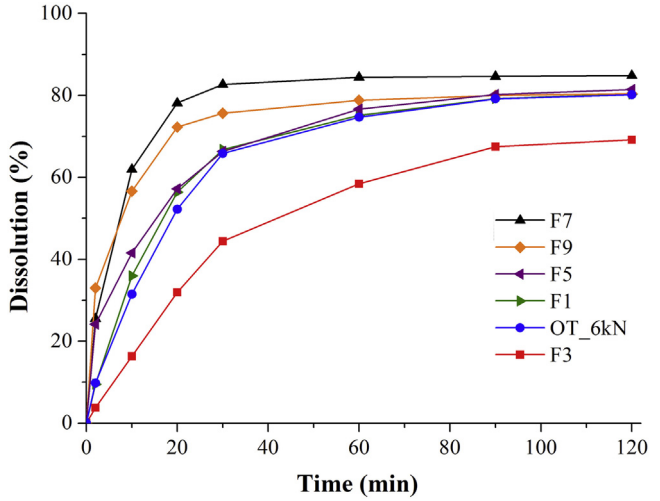

Figure 1. Dissolution profiles of tablets containing ITR-PVPVA64 electrospun solid dispersion and 1% MgSt ($n = 3$). Parameters: USPII, 900 mL of 0.1 N HCl, 100 rpm, 37 ± 0.5°C, 50 mg dose.

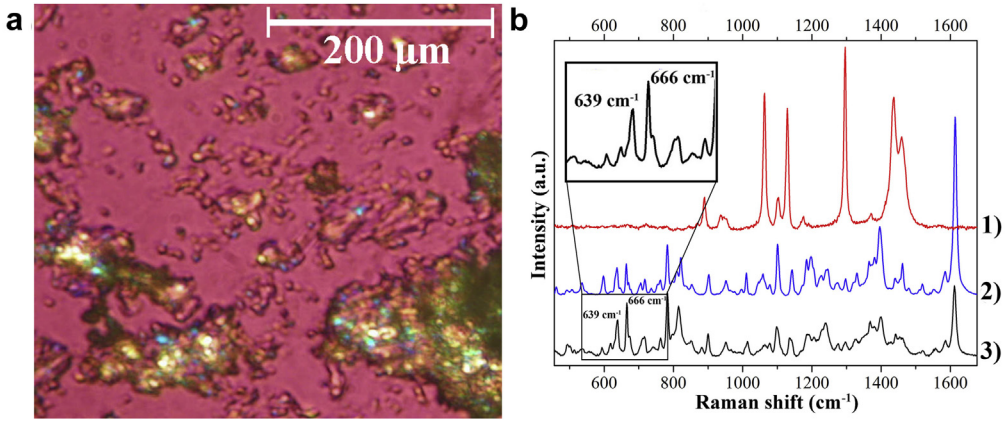

Figure 2. Polarized light microscopy image of filtered sample after dissolution of tablet with (a) MgSt and (b) Raman spectra of (1) MgSt, (2) crystalline ITR, and (3) crystal in the filtered powder.

the latter showed faster disintegration (98 vs. 363 s) despite the fact that direct correlation between disintegration time and dissolution was reported by several authors.[30,31] Consequently, this suggests that dissolution rate is dependent on composition rather than on disintegration time and it is determined by particle size after disintegration. One possible explanation is that dissolution was facilitated in case of F9 by better and faster wetting. Wetting was promoted by 2 factors: more mannitol in the tablet and more MCC generating a significant distance among EM particles (even during dissolution). On the other hand, these MCC aggregates are not disintegrating quickly due to the high compression force applied (MCC particles deform plastically and induce a strong adhesion). However, such visible divergence cannot be observed among F5, F1, and optimal tablets, which had similar dissolution curves in spite of differences in composition and disintegration time. F3 tablets (with low fillers fraction and high compression force) had definitely the lowest dissolution rate and extent.

The Crystallization Phenomenon

Amorphous solid dispersion prepared by high speed electrospinning was reported to release ITR of more than 95% during 20 min and 100% after 60 min.[29] For tablets, dissolution is obviously slower due to the disintegration step before wetting. It was not obvious, however, why the tablets released only ~80% of ITR.

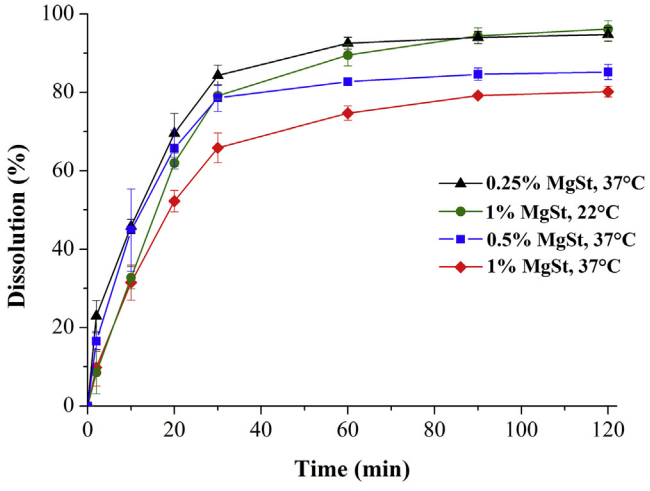

Figure 3. Temperature and lubricant content dependency of ITR dissolution profile ($n = 3$). Parameters: USPII, 900 mL of 0.1 N HCl, 100 rpm, 37 ± 0.5°C, 50 mg dose.

Dissolution extent seems to be somewhat correlated with dissolution rate because F7 tablets exhibited the highest, while F3 the lowest dissolution rate.

Flask measurements were carried out in order to check whether tablets contained the appropriate amount of ITR. The results confirmed that blends and tablets contained 99.85 ± 1.03% and 98.86 ± 1.81% of 50 mg ITR, respectively; therefore no loss of EM has occurred during blending or tableting.

There was a difference between dissolution tests and flask measurements. The previous ones were executed at elevated temperature (37°C), while the flask measurements were executed at room temperature (~22°C). Thus, the temperature dependency of the amount of dissolved ITR was investigated at 4 different temperatures. Interestingly, lower amount of dissolved ITR was observed when the temperature was increased: 101.3 ± 1.52%, 96.4 ± 0.94%, 91.0 ± 1.25%, and 76.5 ± 2.43% at 22°C, 32°C, 37°C, and 45°C, respectively. In these cases, wetting was of course significantly better than during dissolution tests. At higher temperature solubility is supposed to be higher as well. However, these results suggest obvious negative correlation between temperature and extent of dissolved drug, which can indicate that ITR crystallizes during the dissolution tests.

To confirm this concept, a dissolution test was performed at 37°C with a tablet that contained only EM, mannitol, and MgSt, that is, without MCC and crospovidone, the water insoluble crystals which would disturb detection (consequently, no complete dissolution was achieved due to the prolonged disintegration). This experiment was carried out in order to detect crystalline ITR which could be formed during dissolution. The solid material in the vessel was filtered after the test in a glass filter funnel and analyzed by polarized light microscopy (Fig. 2a). PVPVA64 and mannitol dissolved in the dissolution medium (37°C) and were separated by filtration. Images clearly showed the presence of crystalline material. According to the Raman investigations, the material was mixed

Table 3
Dissolution Extent (at 37°C), Tensile Strength, Disintegration Time, and Porosity Comparison of Tablets With Different Lubrication ($n = 3$)

Tablet	Dissolution Extent (%)	Tensile Strength (N/mm^2)	Disintegration Time (s)	Porosity
1% MgSt	80.2 ± 1.4	1.94 ± 0.04	337 ± 36	0.213 ± 0.005
0.5% MgSt	85.2 ± 1.9	2.03 ± 0.04	280 ± 20	0.199 ± 0.004
3% SSF	98.5 ± 2.2	1.61 ± 0.11	438 ± 25	0.204 ± 0.002
1.5% SSF	97.0 ± 2.2	2.16 ± 0.18	443 ± 29	0.210 ± 0.002

Parameters of the dissolution test: USPII, 900 mL of 0.1 N HCl, 100 rpm, 37 ± 0.5°C, 50 mg dose.

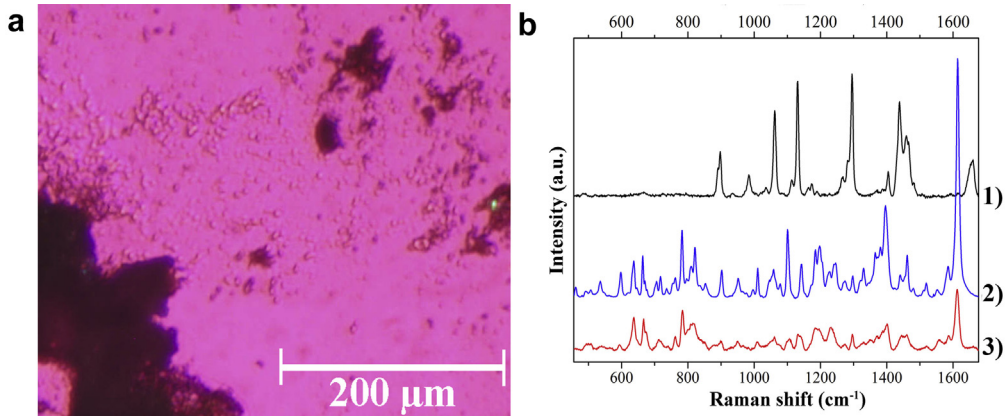

Figure 4. Polarized light microscopy image of filtered sample after dissolution of tablet with (a) SSF and (b) Raman spectra of (1) SSF, (2) crystalline ITR, and (3) filtered powder.

with MgSt and ITR (data not shown). When laser was focused on one crystal by changing the objective to a 100× magnification (spot size ~0.8 µm) crystalline ITR was detected (Fig. 2). If the ratio of peaks at 666 and 639 cm^{-1} of ITR is over 1.05, it means that the examined sample is crystalline.[32] It is clearly visible in the figure that 666 cm^{-1} peak has larger intensity than the peak at 639 cm^{-1}.

The extent of crystallization was not dependent clearly on dissolution rate (and disintegration time) with the tablets from the DoE (Fig. 1) although some correlation can be noticed. An excipient-induced crystallization seemed more likely in this case. MgSt was suspected to induce crystallization as a hydrophobic material. Thus, the goal of our further experiments was to reveal the possible adverse effects.

In subsequent dissolution tests, the following parameters were changed: amount of MgSt (0.25%, 0.5%, and 1%) and temperature of the test (37°C and room temperature 22°C) (Fig. 3).

Tablets with 0.25% MgSt exhibited the fastest dissolution, which can be attributed to rapid wetting in the first 10 min. The compression properties deteriorated, however, at such a low lubricant content. More the MgSt is included in the tablet, the lower dissolution extent is realizable. The effect of the presence of MgSt became clear when dissolutions with SSF containing tablets were carried out (see Tablets With SSF).

The highest extent of dissolved ITR could be achieved when dissolution was performed at 22°C because ITR seemed not to crystallize in this case. This phenomenon can be attributed to 2 temperature-dependent competitive processes: dissolution and crystallization of ITR. Molecular mobility obviously becomes higher with increasing temperature. According to flask measurements, the amount of dissolved ITR is decreasing with rising temperature. Furthermore, an exponential correlation can be observed between the crystallized amount and temperature. Therefore, the kinetics of this crystallization phenomenon might follow the Arrhenius equation. As the temperature is increasing the activation energy of crystallization can be overcome progressively and crystallization becomes more and more prevalent, probably on the hydrophobic surface of MgSt.

Tablets With SSF

In order to achieve higher extent of dissolution (while maintaining good compression properties), MgSt was changed to a less hydrophobic lubricant, SSF. To explore the effect of the new lubricant, concentration of 3% and 1.5% was used as a first and second trial. Dissolution extent, tensile strength, disintegration time, and porosity were checked. As a comparison to tablets with 3% and 1.5% SSF, features of tablets with 1% and 0.5% MgSt are also described (Table 3).

For SSF containing tablets, >95% dissolution could be achieved which is, from pharmaceutical point of view, satisfactory. Rate and extent of dissolution and compression properties were acceptable (data not shown) with both 1.5% and 3% SSF leading to the conclusion that both are applicable in a formulation.

Generally, increasing the porosity of a tablet decreases its mechanical strength and this relationship is sometimes linear.[33] Tablets containing MgSt behaved accordingly. The bonding capacity of particles decreases (and porosity increases) at higher (i.e., 1%) MgSt concentration due to higher coverage of their surface with hydrophobic layer. Tablets with less MgSt (and thus less hydrophobic coverage) disintegrated within a shorter time as water can come into contact with particles faster and more easily. In case of more hydrophilic SSF porosity decreased with increasing lubricant content but the introduction of 3% lubricant yet reduced the tensile strength because of the plasticizing effect of the low molecular weight additive. The water soluble SSF does not affect the wetting and disintegration time significantly. Friability was found to be 0.05% with tablets containing 1.5% SSF. Based on the results blend with 1.5% was chosen for further experiments.

As a reference it was checked whether crystallization takes place during dissolution from tablets containing EM, mannitol, and SSF.

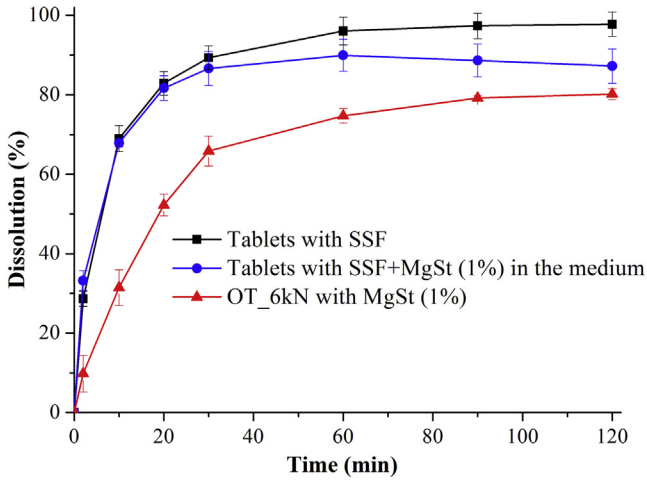

Figure 5. Dissolution from optimal tablets (with SSF) and with additional MgSt powder in the dissolution medium ($n = 3$). Parameters: USPII, 900 mL of 0.1 N HCl, 100 rpm, 37 ± 0.5°C, 50 mg dose.

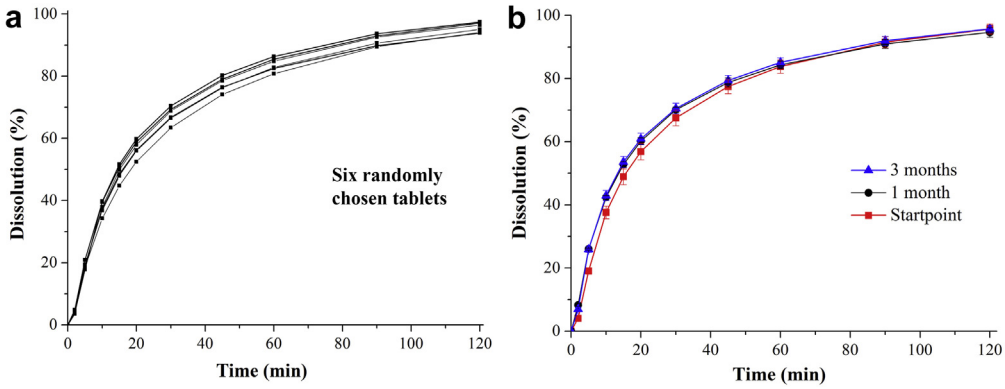

Figure 6. Dissolution of ITR from randomly chosen tablets produced on rotary press (a) and from tablets at starting point and kept at 25°C/60% RH for 1 and 3 months (b). Parameters: USPII, 900 mL of 0.1 N HCl, 100 rpm, 37 ± 0.5°C, 50 mg dose.

Polarized light microscopy images did not show the presence of crystals (Fig. 4).

Polarized light microscopy and Raman spectrometry confirmed that the pure ITR in the filtered material is (measurements of random points of the sample) amorphous: the intensity of peak at 666 cm^{-1} is smaller than that of 639 cm^{-1}, unlike in the spectrum of crystalline ITR (Fig. 4) and sample from MgSt dissolution (Fig. 2). Although 100% dissolution was not achieved due to long disintegration, ITR did not crystallize with SSF in an extent that would be perceivable with microscopy and Raman spectroscopy. On the other hand, ITR in its highly supersaturated state can adsorb onto the surface of MgSt and crystallize there. To confirm this assumption MgSt (equal to 1%) has been added to the dissolution medium of tablets of good dissolution in order to find out whether MgSt induces crystallization. MgSt was put into a basket moving in the vessel. Some of it was floating in course of the test, thus probably less of it was available as a crystallization substrate. The results are shown in Figure 5.

Clearly, MgSt generated crystallization of API although this effect was less extensive than in the cases of MgSt containing formulations. Based on these experiments, MgSt seems to act as nucleation promoting agent for amorphous ITR providing a hydrophobic environment and compromises its advantageous dissolution characteristics. Both the presence of MgSt and elevated temperature (37°C) are required for the crystallization process to occur. The results suggest crystallization of a certain fraction of ITR even at lower doses if the circumstances discussed above are given.

Scaled-Up Tableting on a Rotary Press and Stability Investigation of Tablets

A further investigation of the segregation and feasibility of scaled-up tableting was performed on a rotary press by varying the speed of rotation. At the higher speed (23 rpm) a tensile strength of 2.17 ± 0.22 N/mm^2 was measured and friability could be kept at 0.02%. Furthermore, relative standard deviation of the mass of tablet (20 tablets) even decreased slightly (2.23 to 1.91) with increasing tableting speed.

Advantageous dissolution properties were maintained for the prepared oblong tablets (Fig. 6). All the 6 randomly chosen tablets from rotary press tableting batch released more than 95% of ITR within 2 h (96.1 ± 1.5%) and there was no significant difference in dissolution rates. Furthermore, the tablets kept at 25°C/60% RH for 3 months showed very similar dissolution profiles like those after production. Presumably, phase separation and recrystallization did not happen during the 3-month storage because no change became apparent in dissolution rates and extents.

To investigate the chemical stability of ITR in tablets, HPLC measurements were carried out on samples kept maintained at 25°C/60% RH for 3 months. In crystalline ITR, 0.32 ± 0.04% impurity was observed, which did not increase during downstream processing (mixing with excipients, compression) and storage under controlled conditions: the contamination remained at 0.33 ± 0.05%.

Conclusions

Dissolution characteristics of tablets containing high speed electrospun solid dispersion of ITR and PVPVA64 were investigated in this work. It was found that MgSt lubricant induced crystallization of the drug in course of *in vitro* dissolution. MgSt compromised the dissolution characteristics of ITR and this is expected to occur with some other amorphous APIs. No “spring and parachute” effect was observed; this crystallization process likely starts at the beginning of dissolution and expands to a level determined by API, amount of MgSt, and temperature. Conversely, SSF dissolves in the medium and does not render a possibility for crystallization. Therefore, higher amount of ITR could be dissolved.

The feasibility of scaled-up tableting of EMs was demonstrated. Several important scientific and industrial aspects were assessed on these tablets and found to be excellent. The potential for scaled-up tableting of electrospun materials (along with good physical and chemical stability) renders new possibilities for formulation scientists to address challenges related to poorly water soluble drugs.

Acknowledgments

This work was financially supported by the New Széchenyi Development Plan (TÁMOP-4.2.1/B-09/1/KMR-2010-0002), OTKA research fund (grant numbers K112644 and PD108975), MedInProt Synergy Program, and the János Bolyai Research Scholarship of the Hungarian Academy of Sciences.

References

1. Crowley MM, Zhang F, Repka MA, et al. Pharmaceutical applications of hot-melt extrusion: part I. *Drug Dev Ind Pharm*. 2007;33(9):909-926.
2. Paudel A, Worku ZA, Meeus J, Guns S, Van den Mooter G. Manufacturing of solid dispersions of poorly water soluble drugs by spray drying: formulation and process considerations. *Int J Pharm*. 2013;453(1):253-284.
3. Repka MA, Battu SK, Upadhye SB, et al. Pharmaceutical applications of hot-melt extrusion: part II. *Drug Dev Ind Pharm*. 2007;33(10):1043-1057.
4. Jijun F, Lishuang X, Xiaoli W, et al. Nimodipine (NM) tablets with high dissolution containing NM solid dispersions prepared by hot-melt extrusion. *Drug Dev Ind Pharm*. 2011;37(8):934-944.

5. Modi A, Tayade P. Enhancement of dissolution profile by solid dispersion (kneading) technique. *AAPS PharmSciTech*. 2006;7(3):E87-E92.
6. Fujii M, Okada H, Shibata Y, Teramachi H, Kondoh M, Watanabe Y. Preparation, characterization, and tableting of a solid dispersion of indomethacin with crospovidone. *Int J Pharm*. 2005;293(1):145-153.
7. Leonardi D, Barrera MG, Lamas MC, Salomón CJ. Development of prednisone: polyethylene glycol 6000 fast-release tablets from solid dispersions: solid-state characterization, dissolution behavior, and formulation parameters. *AAPS PharmSciTech*. 2007;8(4):221-228.
8. Dhumal R, Shimpi S, Paradkar A. Development of spray-dried co-precipitate of amorphous celecoxib containing storage and compression stabilizers. *Acta Pharm*. 2007;57(3):287-300.
9. Soulairol I, Tarlier N, Bataille B, Cacciaguerra T, Sharkawi T. Spray-dried solid dispersions of nifedipine and vinylcaprolactam/vinylacetate/PEG 6000 for compacted oral formulations. *Int J Pharm*. 2015;481(1):140-147.
10. Patel M, Patel D. Fast dissolving valdecoxib tablets containing solid dispersion of valdecoxib. *Indian J Pharm Sci*. 2006;68(2):222-226.
11. Chaulang G, Patil K, Ghodke D, Khan S, Yeole P. Preparation and characterization of solid dispersion tablet of furosemide with crospovidone. *Res J Pharm Tech*. 2008;1(4):386-389.
12. Mohammed NN, Majumdar S, Singh A, et al. Klucel™ EF and ELF polymers for immediate-release oral dosage forms prepared by melt extrusion technology. *AAPS PharmSciTech*. 2012;13(4):1158-1169.
13. Borbás E, Balogh A, Bocz K, et al. In vitro dissolution–permeation evaluation of an electrospun cyclodextrin-based formulation of aripiprazole using μFlux™. *Int J Pharm*. 2015;491(1–2):180-189.
14. Augustijns P, Brewster ME. Supersaturating drug delivery systems: fast is not necessarily good enough. *J Pharm Sci*. 2012;101(1):7-9.
15. Six K, Daems T, de Hoon J, et al. Clinical study of solid dispersions of itraconazole prepared by hot-stage extrusion. *Eur J Pharm Sci*. 2005;24(2–3):179-186.
16. Bevernage J, Brouwers J, Brewster ME, Augustijns P. Evaluation of gastrointestinal drug supersaturation and precipitation: strategies and issues. *Int J Pharm*. 2013;453(1):25-35.
17. Kostewicz ES, Abrahamsson B, Brewster M, et al. In vitro models for the prediction of in vivo performance of oral dosage forms. *Eur J Pharm Sci*. 2014;57:342-366.
18. Démuth B, Nagy Z, Balogh A, et al. Downstream processing of polymer-based amorphous solid dispersions to generate tablet formulations. *Int J Pharm*. 2015;486(1):268-286.
19. Vandecruys R, Peeters J, Verreck G, Brewster ME. Use of a screening method to determine excipients which optimize the extent and stability of supersaturated drug solutions and application of this system to solid formulation design. *Int J Pharm*. 2007;342(1–2):168-175.
20. Fathima N, Mamatha T, Qureshi HK, Anitha N, Rao JV. Drug-excipient interaction and its importance in dosage form development. *J Appl Pharm Sci*. 2011;1(6):66-71.
21. Fraser Steele D, Edge S, Tobyn MJ, Christian Moreton R, Staniforth JN. Adsorption of an amine drug onto microcrystalline cellulose and silicified microcrystalline cellulose samples. *Drug Dev Ind Pharm*. 2003;29(4):475-487.
22. Richards RME, Xing JZ, Mackay KM. Excipient interaction with cetylpyridinium chloride activity in tablet based lozenges. *Pharm Res*. 1996;13(8):1258-1264.
23. Nagy ZK, Balogh A, Drávavölgyi G, et al. Solvent-free melt electrospinning for preparation of fast dissolving drug delivery system and comparison with solvent-based electrospun and melt extruded systems. *J Pharm Sci*. 2013;102(2):508-517.
24. Balogh A, Drávavölgyi G, Faragó K, et al. Plasticized drug-loaded melt electrospun polymer mats: characterization, thermal degradation, and release kinetics. *J Pharm Sci*. 2014;103(4):1278-1287.
25. Mickova A, Buzgo M, Benada O, et al. Core/shell nanofibers with embedded liposomes as a drug delivery system. *Biomacromolecules*. 2012;13(4):952-962.
26. Jiang YN, Mo HY, Yu DG. Electrospun drug-loaded core-sheath PVP/zein nanofibers for biphasic drug release. *Int J Pharm*. 2012;438(1–2):232-239.
27. Yu DG, Li XY, Wang X, Yang JH, Bligh SA, Williams GR. Nanofibers fabricated using triaxial electrospinning as zero order drug delivery systems. *ACS Appl Mater Inter*. 2015;7(33):18891-18897.
28. Han D, Steckl AJ. Triaxial electrospun nanofiber membranes for controlled dual release of functional molecules. *ACS Appl Mater Inter*. 2013;5(16):8241-8245.
29. Nagy ZK, Balogh A, Demuth B, et al. High speed electrospinning for scaled-up production of amorphous solid dispersion of itraconazole. *Int J Pharm*. 2015;480(1-2):137-142.
30. Zhao N, Augsburger LL. Functionality comparison of 3 classes of superdisintegrants in promoting aspirin tablet disintegration and dissolution. *AAPS PharmSciTech*. 2005;6(4):E634-E640.
31. Gohel MC, Parikh RK, Brahmbhatt BK, Shah AR. Improving the tablet characteristics and dissolution profile of ibuprofen by using a novel coprocessed superdisintegrant: a technical note. *AAPS PharmSciTech*. 2007;8(1):E94-E99.
32. Démuth B, Farkas A, Pataki H, et al. Detailed stability investigation of amorphous solid dispersions prepared by single-needle and high speed electrospinning. *Int J Pharm*. 2016;498(1–2):234-244.
33. Ryshkewitch E. Compression strength of porous sintered alumina and zirconia. *J Am Ceram Soc*. 1953;36(2):65-68.